

## ELECTRONIC SUPPLEMENTARY INFORMATION

### **A reusable magnetic nanocatalyst for bio-fuel additives: The ultrasound-assisted synthesis of solketal**

Kalyani Rajkumari,<sup>a</sup> Bishwajit Changmai,<sup>a</sup> Ananta Kumar Meher,<sup>a</sup> Chhangte Vanlalveni,<sup>b</sup> Putla Sudarsanam,<sup>c</sup> Andrew E. H. Wheatley,<sup>\*d</sup> Samuel Lalthazuala Rokhum<sup>\*a,d</sup>

<sup>a</sup>Department of Chemistry, National Institute of Technology Silchar, Assam-788010, India

<sup>b</sup>Department of Botany, Mizoram University, Tanhril, Aizawl, Mizoram, 796001, India

<sup>c</sup>Catalysis and Inorganic Chemistry Division, CSIR-National Chemical Laboratory, Dr Homi Bhabha Road, Pune 411008, India

<sup>d</sup>Yusuf Hamied Department of Chemistry, University of Cambridge, Lensfield Road, Cambridge CB2 1EW, UK

\*Corresponding authors. Tel.: +91 3842 242915; fax: +91 3842-224797; Email address: aehw2@cam.ac.uk (AEHW); lr512@cam.ac.uk, rokhum@che.nits.ac.in (SLR)

## Table of contents

Section	Content	Graphic
1.	XPS survey spectrum of FSS MNP catalyst	Figure S1
2.	Analytical data for the product of glycerol acetalization by FSS MNP catalyst <ul style="list-style-type: none"> <li>- <math>^1\text{H}</math> and <math>\{^1\text{H}\}^{13}\text{C}</math> NMR spectra</li> <li>- GC data</li> </ul>	Figure S2 Figure S3
3.	Mechanism of acetalization of glycerol <ul style="list-style-type: none"> <li>- Proposed mechanism using FSS MNP catalyst</li> </ul>	Scheme S1
4.	Activation energy data <ul style="list-style-type: none"> <li>- Plot of <math>\ln k</math> vs. <math>1/T \times 10^3</math> (<math>\text{K}^{-1}</math>) for a ultrasonically-assisted synthesis</li> <li>- Plot of <math>\ln k</math> vs. <math>1/T \times 10^3</math> (<math>\text{K}^{-1}</math>) for a magnetically-stirred synthesis</li> </ul>	Figure S4 Figure S5
5.	Procedure for the scaled-up acetalization of glycerol	–
6.	Analysis of FSS MNP catalyst after 5 recycling experiments <ul style="list-style-type: none"> <li>- FTIR spectra</li> <li>- EDX data</li> <li>- Room temperature magnetization curve</li> <li>- Representative TEM images</li> <li>- Particle size distribution histogram (<math>N = 100</math>)</li> </ul>	Figure S6 Figure S7 Figure S8 Figure S9 Figure S10
7.	TON and TOF calculations	–
8.	References	–

## 1. XPS survey spectrum of FSS MNP catalyst

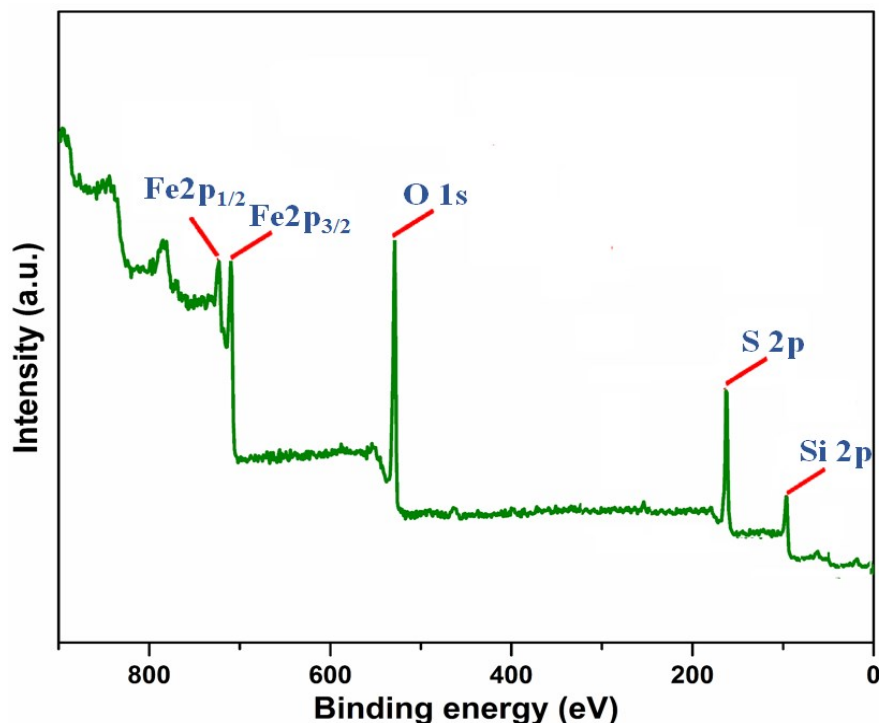
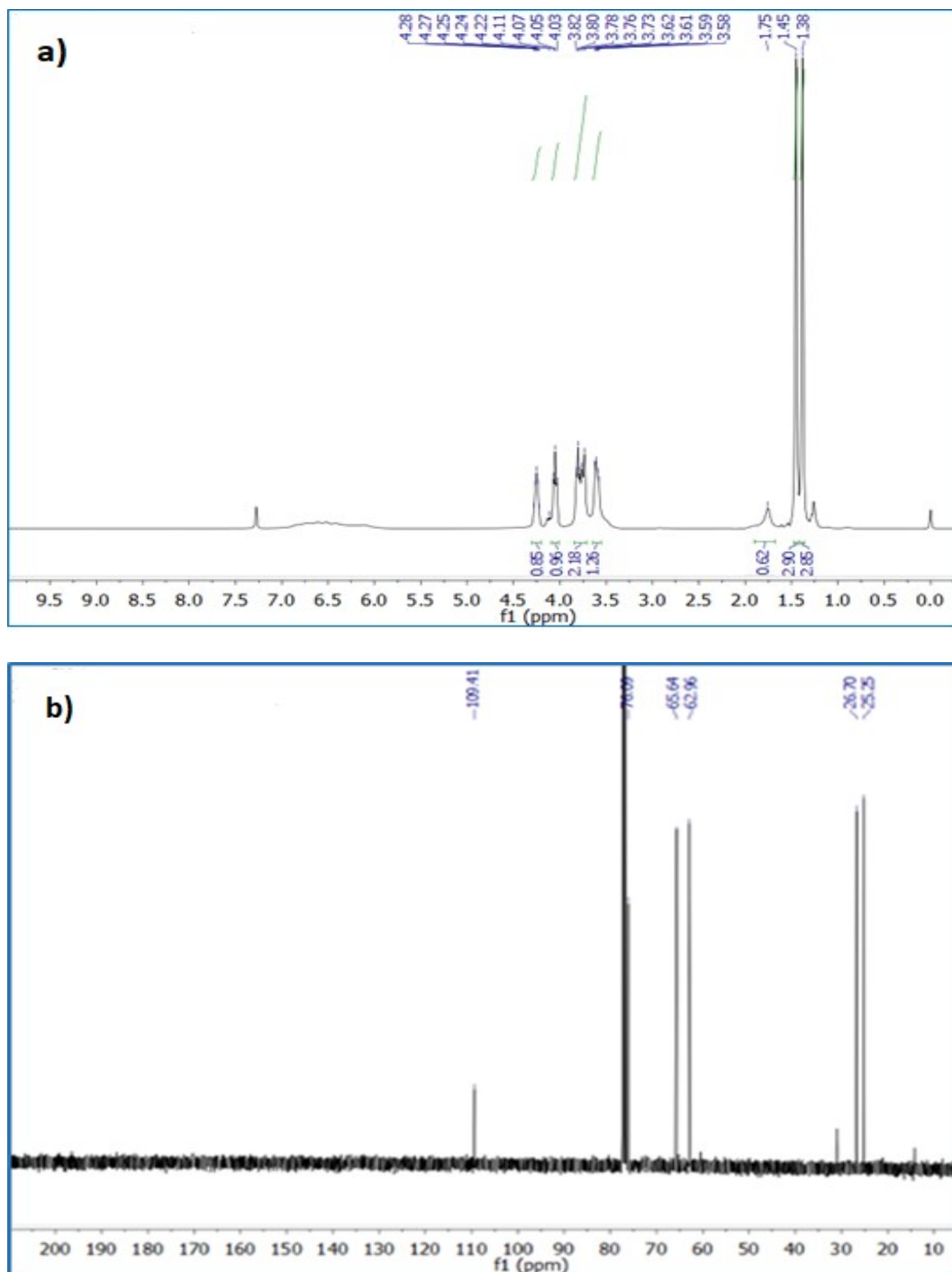


Figure S1: XPS survey spectrum of FSS MNPs.

## 2. Analytical data for the product of glycerol acetalization by FSS MNP catalyst

In the  $^1\text{H}$  NMR spectrum of the product of glycerol acetalization (Figure S2a) the two distinct singlets at  $\delta$  1.38 and  $\delta$  1.45 refer to the six methyl hydrogens of 1,3-dioxolane product while the broad singlet peak for hydroxyl appears at  $\delta$  1.75. Peaks in the region  $\delta$  3.58-4.28 have a total integration of five and represent the  $-\text{CH}_2$  and  $-\text{CH}$  groups present in the product structure. The  $^{13}\text{C}$  NMR spectrum of the solketal product is shown in Figure S2b. The most shielded peaks, at  $\delta$  25.3 and  $\delta$  26.7, are due to the methyl carbons. The peak at  $\delta$  76.1 is due to the  $-\text{CH}$  carbon and the other two peaks at  $\delta$  65.6 and 63.0 refer to the two  $-\text{CH}_2$  carbons. The most deshielded peak, at  $\delta$  109.4, is due to the ketal carbon. These two spectra clearly provide evidence for the formation of 5-membered solketal product,<sup>1</sup> pointing to it being the sole product, of glycerol acetalization. The absence of NMR peaks due to the previously reported six-membered acetal (2,2-dimethyl-1,3-dioxan-5-ol) argue against the competitive formation of the corresponding 6-membered acetal ring in the reaction.<sup>2</sup>  $^1\text{H}$  and  $\{^1\text{H}\}^{13}\text{C}$  NMR spectra recorded on Bruker Avance II, 400 MHz

spectrometer at 28 °C. Deuterated solvent stored over molecular sieves (3 Å). Chemical shifts ( $\delta$  ppm) internally referenced to deuterated solvent and calculated relative to TMS.



**Figure S2:** (a)  $^1\text{H}$  NMR (400 MHz) and (b)  $\{^1\text{H}\}^{13}\text{C}$  NMR (100 MHz) spectra in  $\text{CDCl}_3$  of the product of glycerol acetalization using FSS MNP catalyst.

GC data recorded on an Agilent 7890 fitted with head-space injector mode, a CPSIL 8CB capillary column (30 m × 0.25 mm × 0.25 μm) and GC FID detector. Initial oven temperature 55 °C. This was increased to 230 °C at 10 °C min<sup>-1</sup>. Temperature of detector and the injector were 300 °C and 250 °C, respectively. Biphenyl used as internal standard.

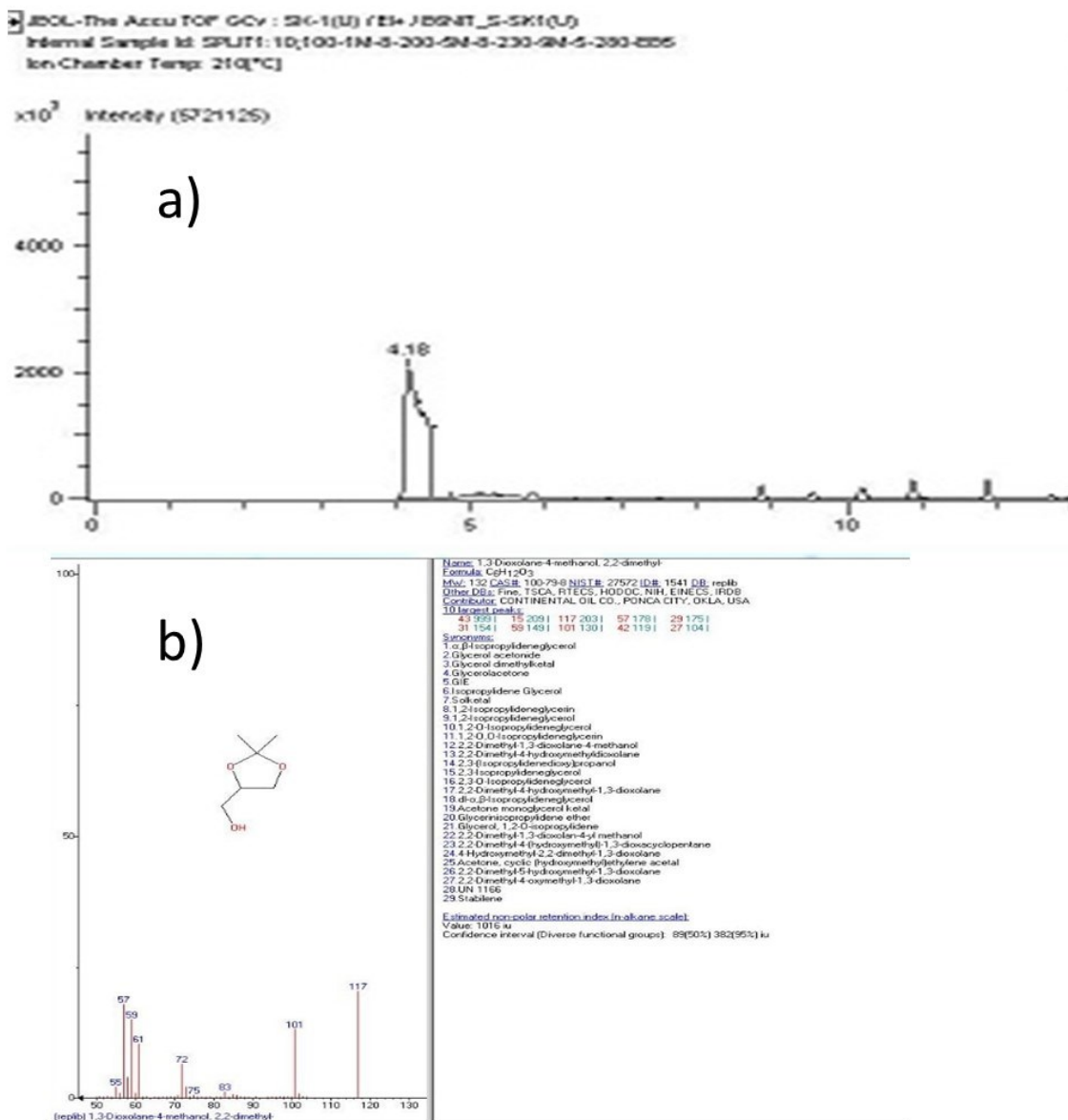
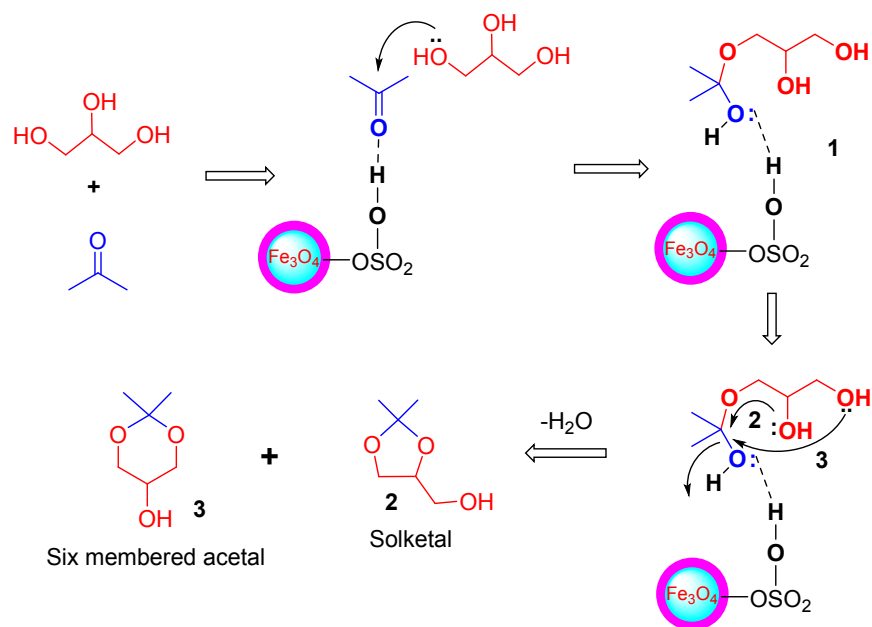


**Figure S3:** a) GC data for synthesized solketal revealing its elution at 4.18 min. The potentially competing 6-membered cyclic acetal would be expected at 7 min. Biphenyl internal standard, oven temperature 55-230 °C, ramp rate 10 °C min<sup>-1</sup>; b) MS spectra of solketal

### 3. Mechanism of acetalization of glycerol

The usual explanation for the selectivity of acetalization is the ketal mechanism.<sup>2,3,4</sup> It is suggested that in our work the first step of the reaction sees the acetone activated by the acid sites of the FSS catalyst to form **1**. This intermediate would then cyclize to form solketal **2** and/or 6-membered cyclic **3**. It is established that formation of **3** is not favorable kinetically,<sup>3</sup> so reaction normally prefers **2**. In our case, the selectivity for **2** over **3** is 100%, i.e. **2** is made to the complete exclusion of **3**.



**Scheme S1:** Proposed mechanism of acetalization of glycerol using FSS MNP catalyst.

#### 4. Activation energy data

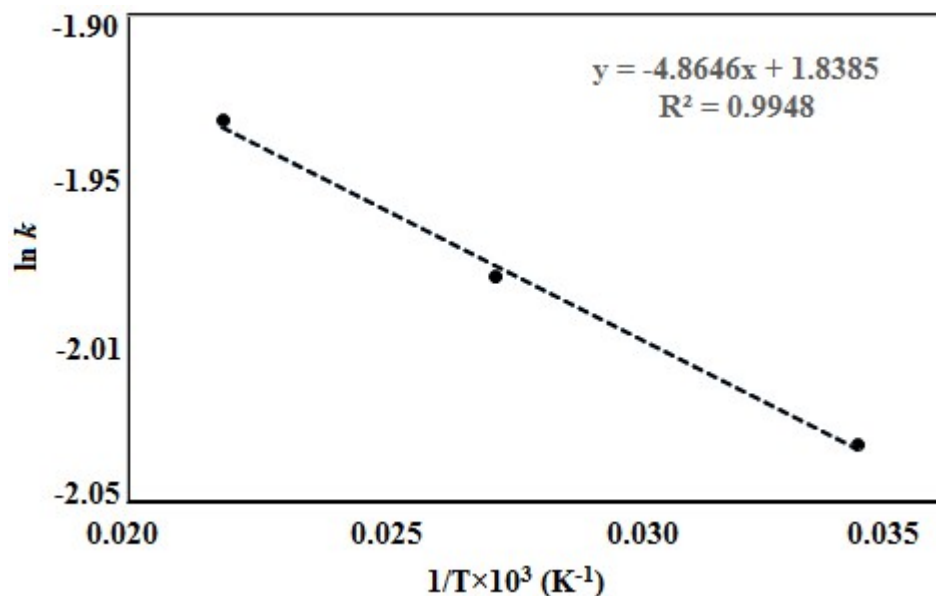


**Figure S4:** Plot of  $\ln k$  vs  $1/T \times 10^3 \text{ (K}^{-1}\text{)}$  for the ultrasonic-assisted synthesis of solketal using FSS MNPs. Reaction conditions: 5:1 acetone/glycerol molar ratio, 2 wt. % catalyst loading, 15 min time.

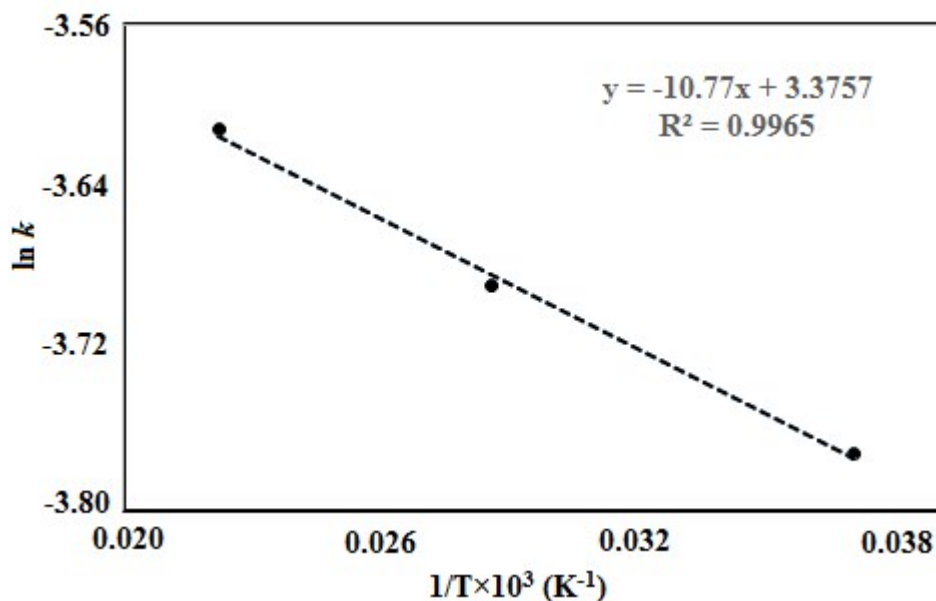


**Figure S5:** Plot of  $\ln k$  vs  $1/T \times 10^3 \text{ (K}^{-1}\text{)}$  for the traditional synthesis of solketal using FSS MNPs. Reaction conditions: 5:1 acetone/glycerol molar ratio, 2 wt. % catalyst loading, 60 min time and 1000 rpm.

## 5. Procedure for the scaled-up acetalization of glycerol

The optimized glycerol acetalization (see main manuscript) was undertaken treating 20 g glycerol (217.3 mmol) and 100 g acetone (1087 mmol) with 1 g of FSS MNP catalyst. Ultrasonication for 15 mins. at 28 °C was followed by catalyst removed using magnetic separation. Centrifugation (3000 rpm for 5 min), removal of excess acetone by rotary evaporation and finally elution of the product (using 8:2 hexane-ethyl acetate solution) in a short alumina column gave solketal (with 100% selectivity) in an isolated yield of 94±1%.

## 6. Analysis of FSS MNP catalyst after 5 recycling experiments

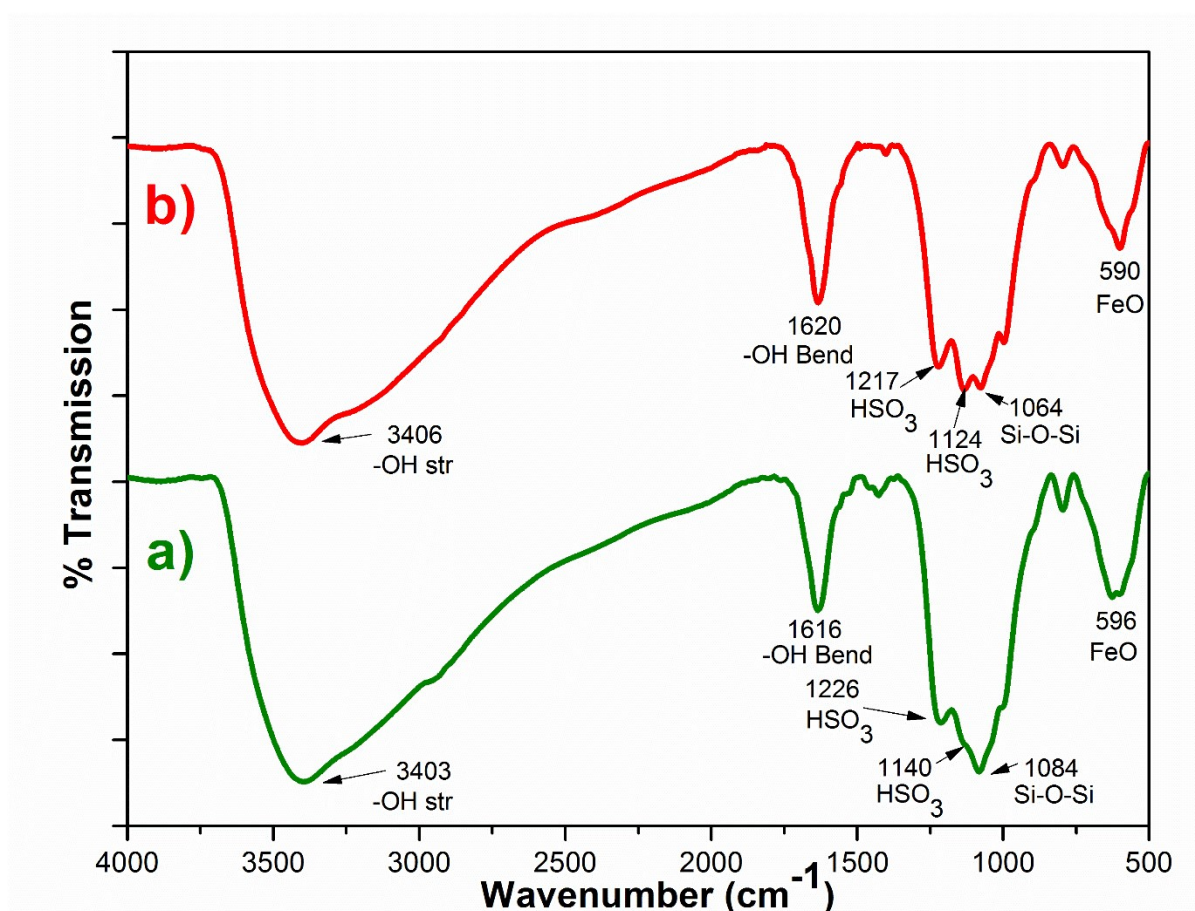


**Figure S6:** FTIR spectra of a) FSS MNPs recovered after 5 catalytic cycles and b) fresh FSS MNPs



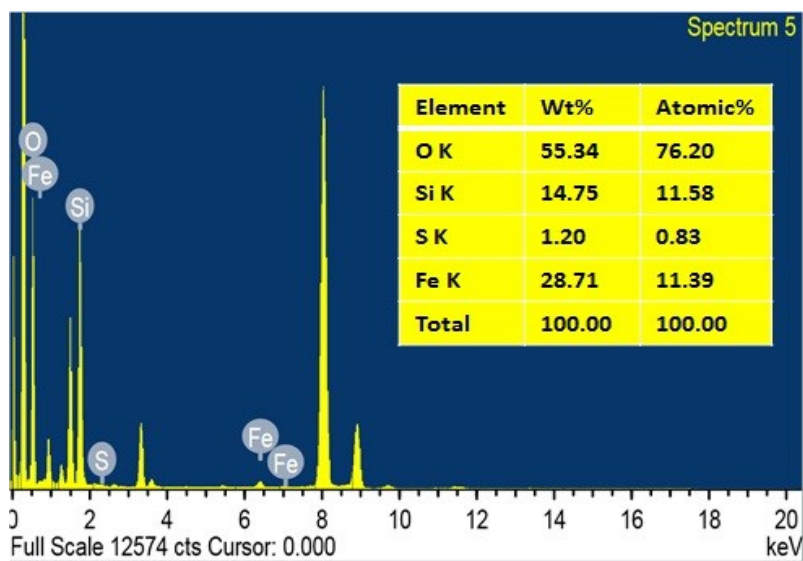


**Figure S7:** EDX data for FSS MNPs recovered after 5 catalytic cycles. Signals at 8.034 and 8.895 keV are due to the Cu grid

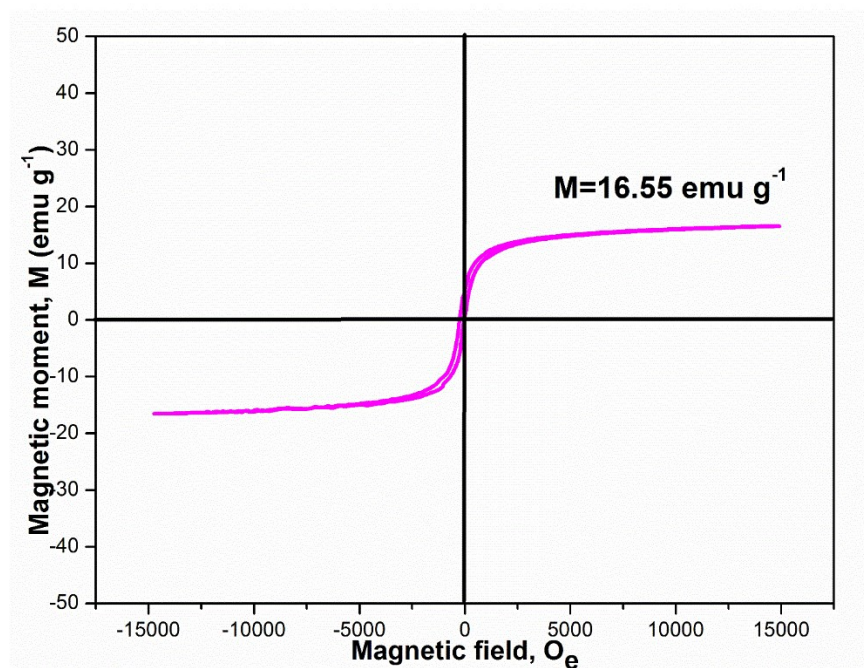


**Figure S8:** Room temperature magnetization curve of FSS MNPs recovered after 5 catalytic cycles

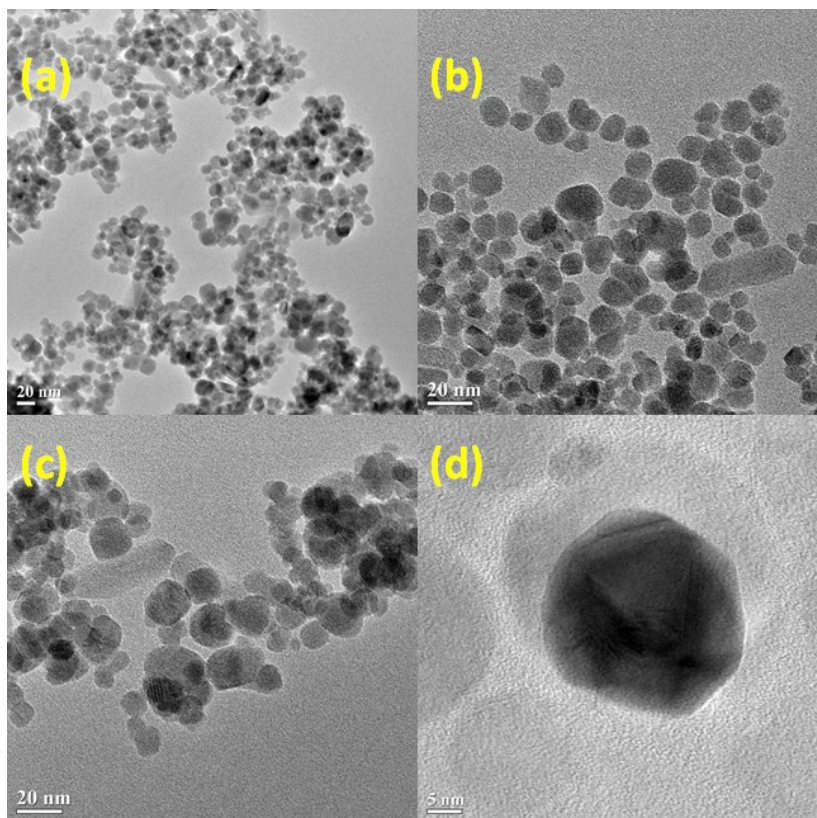


**Figure S9:** Representative TEM images of FSS MNPs recovered after 5 catalytic cycles. Scale bars 20 nm (a-c) and 5 nm (d)

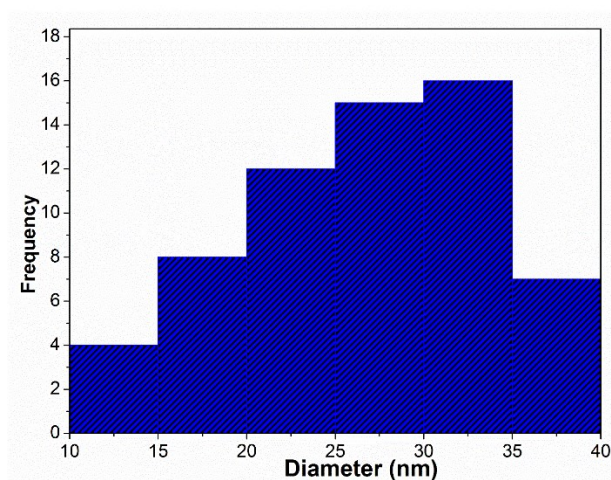


**Figure S10:** Particle size distribution histogram for FSS MNPs recovered after 5 catalytic cycles (N = 100)

## 6. Turnover number (TON) and Turnover frequency (TOF) Calculation

TOF = TON/time of reaction

$$\text{TON} = \frac{\% \text{ Conversion of glycerol}}{(\text{Catalyst wt.}\%)(\text{Molar mass glycerol})}$$

$$\text{TOF} = \frac{\% \text{ Conversion of glycerol}}{(\text{Time})(\text{Catalyst wt.}\%)(\text{Molar mass glycerol})}$$

## 7. References

1. I. B. Laskar, K. Rajkumari, R. Gupta and L. Rokhum, *Energy Fuels*, 2018, **32**, 12567-12576.
2. C. Crotti, E. Farnetti and N. Guidolin, *Green Chem.*, 2010, **12**, 2225-2231.
3. B. Mallesham, P. Sudarsanam, G. Raju and B. M. Reddy, *Green Chem.*, 2013, **15**, 478-490.
4. A. R. Trifoi, S. P. Agachi and T. Pap, *Renewable Sustainable Energy Rev.*, 2016, **62**, 804-814.